

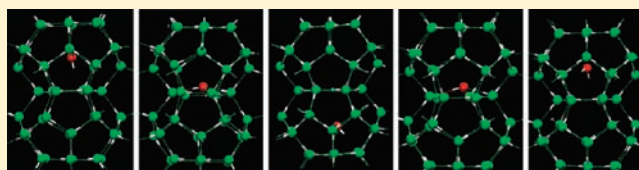
The Mobility of Water Molecules through Gas Hydrates

Shuai Liang and Peter G. Kusalik*

Department of Chemistry, University of Calgary, 2500 University Drive NW, Calgary, Alberta, Canada

S Supporting Information

ABSTRACT: Crystal growth simulations of gas hydrates have suggested that hydrate cages may occasionally be occupied by H₂O rather than guest molecules, leaving interstitial defects within the hydrate crystal. Further inspection of the behavior of these interstitial H₂O molecules has revealed that they are relatively highly mobile entities within a gas hydrate. In this paper, we report these observations and examine the molecular mechanisms responsible for the transport of these interstitial molecules through hydrate crystals. Four distinct pathways for the H₂O molecule transport between cages are found, each facilitated by the presence of empty cages. The relative richness of the observed behavior of interstitial defects suggests that interstitial diffusion could be an important mechanism for the mass transport of H₂O molecules through gas hydrates.



An interstitial water molecule hopping between hydrate cages

Four distinct pathways for the H₂O molecule transport between cages are found, each facilitated by the presence of empty cages. The relative richness of the observed behavior of interstitial defects suggests that interstitial diffusion could be an important mechanism for the mass transport of H₂O molecules through gas hydrates.

1. INTRODUCTION

Gas hydrates are crystalline compounds with guest–host structures, in which gas molecules are trapped in hydrogen-bonded water cages.¹ Gas hydrates have received intense interest in the scientific and industrial fields because of their relevance in hydrocarbon extraction,^{2,3} carbon dioxide sequestration,^{4,5} energy storage,^{6–8} global warming,^{9–12} marine geohazards,^{13,14} etc. The understanding of gas hydrate formation is potentially crucial for energy recovery and storage as well as flow assurance in oil and natural gas pipelines.

Typically, experimental investigations of hydrate formation are performed by exposure of a liquid H₂O or ice phase to (gaseous) guest molecules.^{15–18} Nucleation of gas hydrates typically takes place at H₂O/gas interfaces where the concentration of both gas and H₂O molecules are relatively high. Once formed, the hydrate films effectively separate the gas and H₂O phases by providing a barrier to mass transfer between them. Thus further hydrate growth requires either effective transport of gas molecules through the hydrate film to the hydrate/H₂O interface or H₂O molecules transfer through the hydrate film to the hydrate/gas interface. A similar situation will occur when liquid CO₂ might be injected into the deep sea.^{4,5} CO₂ hydrates tend to form at the interface between liquid CO₂ and water. The presence of hydrates would affect the mass transfer of the CO₂ or H₂O molecules and consequently limits the growth rate of hydrates at the interface.

Controversy exists about whether the transport of the gas^{16,19,20} or H₂O^{21,22} molecules controls hydrate growth rates. Monte Carlo simulations with a Landau free energy method have suggested a significantly higher diffusion coefficient (10^{−12} m²/s) for CO₂ molecules relative to that for H₂O molecules (10^{−23} m²/s) in hydrates.²³ Path sampling calculation have also suggested a relatively large diffusion coefficient (10^{−16} m²/s) for CH₄ in hydrates.²⁴ Infrared spectroscopic studies of hydrate formation have revealed that three different ethers can form hydrates at similar rates despite differences in the size and shapes of these guest molecules,¹⁵ which suggests that hydrate formation is dominated by H₂O

mobility rather than gas diffusion. In addition, recent high-resolution confocal Raman spectroscopy has provided more direct evidence that H₂O molecules are the most mobile species in the hydrate phase, and hydrate growth is controlled by the diffusion of H₂O within the hydrate films.²⁵

Despite its (their) importance in understanding the growth behavior of hydrate films at H₂O/gas interfaces, the molecular mechanism(s) of mass transport through hydrate crystals remain(s) unclear. Since molecules in a perfect crystalline solid are generally immobilized by strong intermolecular interactions and dense packing, the hopping of molecules through rings of the intact host lattice would face substantial energy barriers. It has been suggested that gas diffusion is assisted by the presence of defects in crystalline structures.²³ The energy barrier for gas molecule passage between a full and empty cage was shown to be reduced substantially by the presence of a H₂O (lattice) vacancy that generates an enlarged “hole” in the cage wall.^{15,23,24} The displacement of such vacancy defects in the host lattice was proposed as a means for H₂O transport. Interstitial H₂O molecules have also been introduced into the host lattice of a CO₂ hydrate;¹⁵ it was found that interstitials can significantly promote the mobility of H₂O molecules to a rate about 2–3 times faster than vacancies. Other mechanisms like Bjerrum defect assisted diffusion²⁶ and crystal decomposition–reconstruction mechanisms^{27,28} have also been suggested.

Our previous molecular dynamics (MD) simulations of gas hydrate crystal growth have revealed that hydrate cages occupied by H₂O rather than guest molecules can form under a variety of conditions as well as with different guest molecules. These systems include H₂S hydrates grown from an aqueous solution with no gas supersaturation (three-phase simulation) or with moderate gas supersaturation (two-phase simulation)^{29,30} and CH₄ hydrates grown from an aqueous

Received: September 17, 2010

Published: January 19, 2011

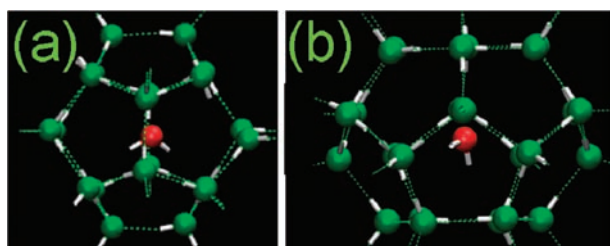


Figure 1. An example of H₂O occupied (a) 5¹² and (b) 5¹²6² cages. H₂O molecules are represented by a sphere for the oxygen and two white sticks for the hydrogens. The oxygens of the host and interstitial H₂O molecules are colored as green and red, respectively. Hydrogen bonds (dotted lines) are defined by the geometric constraints that $d_{\text{O}-\text{O}} < 3.0 \text{ \AA}$ and $\angle \text{O}-\text{H}\cdots\text{O} < 20^\circ$.

solution with a highly elevated CH₄ composition.^{31,32} The appearance of this defect structure was also independent of the ensemble (NVE, NVT, NPT) being employed in the simulation. Figure 1 shows examples of a H₂O molecule trapped in a 5¹² and a 5¹²6² cage of a structure I (sI) CH₄ hydrate. A subsequent careful inspection of these interstitial H₂O molecules revealed that these molecules do not typically remain in one specific cage for a long time; rather they appear able to “hop” to neighboring cages.

In this paper, we explore these observations of water transport through gas hydrate crystals and probe the molecular mechanisms responsible for the mobility of interstitial H₂O molecules. Four typical transport paths, all involving interstitial H₂O molecules moving to vacant cages, were observed directly within our MD simulations of gas hydrates. We demonstrate that these paths could represent means by which H₂O molecules transport through hydrate crystals relatively easily. An estimation of an effective diffusion constant is consistent with recent experimental observations²⁵ that suggest that H₂O molecules are the most mobile species in the hydrate phase.

2. METHODOLOGY

While the molecular mechanisms of the transport of interstitial H₂O molecules through CH₄ and H₂S hydrates are found qualitatively to be very similar, we will focus our detailed analyses on the transport of interstitial H₂O defects through a CH₄ hydrate crystal; the corresponding behavior within a H₂S hydrate is reported in the Supporting Information (SI).

The starting configurations for the present simulations, each containing a single interstitial defect, consisted of a periodic two-phase system, where a CH₄ hydrate crystal was in contact with an aqueous CH₄ solution. These configurations were taken directly from crystal growth simulations in which such a defect had appeared. MD simulations were performed at constant pressure and constant temperature (NPT ensemble) at a pressure of 50 MPa and temperatures of 265 and 275 K. Data were also collected at temperatures of 255 and 245 K but were more limited. The length of each simulation was 12 ns (limited in part by the lifetime of the interstitial defect in the crystal since it disappears when it reaches a hydrate/liquid interface). Additional details of the models and simulation methodology used in this work, which have been used extensively to study the crystal growth of gas hydrates, can be found in the SI.

While we did not observe differences in the H₂O transport mechanisms in the 12 ns simulation at each temperature, all the examples given in section 3 are from the simulation run at 265 K. Unless otherwise noted, the molecular coordinates and potential energies reported in this work are averaged over a time window of 1 ps. Values averaged over a much shorter time window of 100 fs were also collected and analyzed to help clarify the observed molecular mechanisms.

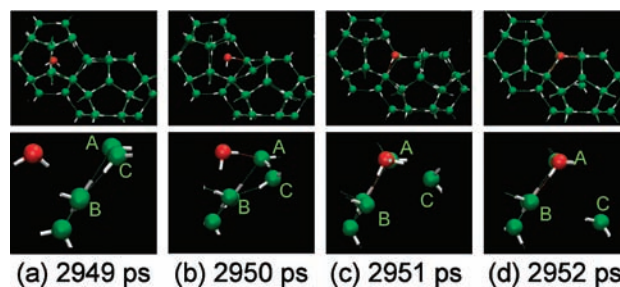


Figure 2. (a–d) Molecular configurations (top) and corresponding ring structures (bottom) showing the mechanism of H₂O molecule transport from a 5¹² cage to a neighboring 5¹²6² cage via replacement of a H₂O molecule in the shared five-membered ring. The corresponding time indexes for these configurations are given in the legends. The molecular coordinates were averaged over 1 ps, and the H₂O molecules are represented as in the case of Figure 1. The molecular labels “A”, “B”, and “C” are discussed in the text.

3. RESULTS AND DISCUSSION

3.1. Transport via Five-Membered Rings. In this subsection, we will identify two different transport mechanisms of interstitial H₂O molecules via replacement of molecules in five-membered rings of a hydrate crystal. Figure 2 shows an example of H₂O transport by bridging across a five-membered ring. The interstitial H₂O molecule originally resides within a 5¹² cage, which has an empty 5¹²6² neighbor cage (Figure 2a). At some point later in the trajectory, we find that this interstitial molecule forms H-bonds to two second-neighbor molecules (“A” and “B”, as labeled in Figure 2b) of a five-membered ring that is shared by the 5¹² and 5¹²6² cages. We see that this interstitial molecule attains a position essentially equivalent to molecule “C” of the ring. Since such a structure is transient (i.e., it does not represent a free energy minimum at this temperature, but it is stable at very low temperatures; see SI), either the interstitial molecule or molecule “C” should leave. If molecule “C” departs (Figure 2c), this event becomes a replacement of a H₂O molecule of the five-membered ring by the interstitial H₂O molecule, with the net result of this process being a H₂O molecule transported from the 5¹² to the 5¹²6² cage. The subsequent structural relaxation of the related molecules reforms the hydrate crystalline structure, now leaving the interstitial defect in the 5¹²6² cage (Figure 2d).

The potential energy contributions (to the system total) of the original and resultant interstitial H₂O molecules during the transport process are shown in Figure 3a, where the potential energy has been averaged over time windows of 1 ps. From this coarse grain data, we can see that the energy decrease of the original molecule and the energy increase of the resultant molecule occur at roughly the same time. This suggests that, during the replacement process, the destabilization of the leaving molecule (due to H-bond weakening or breaking) is essentially compensated for by the stabilization of the incoming molecule. This is consistent with the behavior seen at very low temperatures (20 K) where the transition (bridged) structure shown in Figure 2b is actually the most stable structure (see SI). The relatively symmetric changes of the potential energies of the two molecules suggest that at this temperature there is a significant entropic contribution to the free energy barrier for this transport process. Figure 3b shows an example of a transport event with higher temporal resolution. While details of the energetic behavior varies for each particular event (e.g., in Figure 3b an energetic plateau is apparent), such replacement (transport)

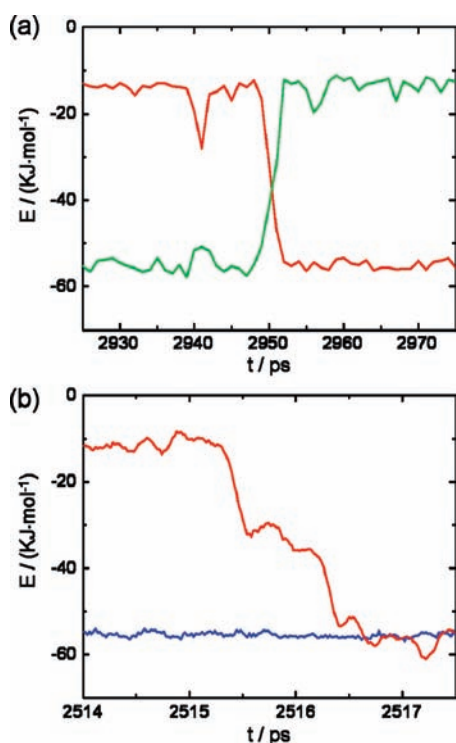


Figure 3. (a) Potential energy (averaged over 1 ps) of the original (red) and resultant (green) interstitial H₂O molecules corresponding to the replacement process shown in Figure 2. (b) Another similar replacement process with the potential energies averaged over 100 fs (with points given every 20 fs). The red line is as that in (a), and the blue line corresponds to the averaged potential energy of the other 38 molecules from the two cages.

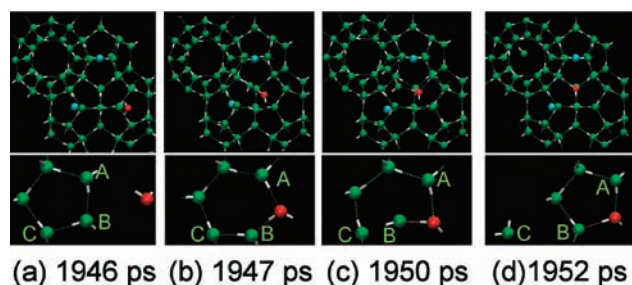


Figure 4. (a–d) Molecular configurations (top) and corresponding ring structures (bottom) showing the mechanism of H₂O molecule transport from a $S^{12}6^2$ cage to a second-neighbor $S^{12}6^2$ cage via replacement of a H₂O molecule in the connecting five-membered ring. The corresponding time indexes for these configurations are given in the legends. H₂O molecules are represented as in the case of Figure 1. The light blue spheres represent CH₄ molecules. The molecular labels “A”, “B”, and “C” are discussed in the text.

processes are typically fast, occurring over only a couple of picoseconds, although on a few occasions we have observed relatively slow events spanning 5–10 ps.

Figure 4 presents another possible path for interstitial H₂O molecule transport; in this case a six-membered ring is formed from the original five-membered ring. The interstitial H₂O molecule is originally in a $S^{12}6^2$ cage, which is connected to another empty $S^{12}6^2$ cage by a five-membered ring (see Figure 4a). This interstitial molecule inserts itself between two

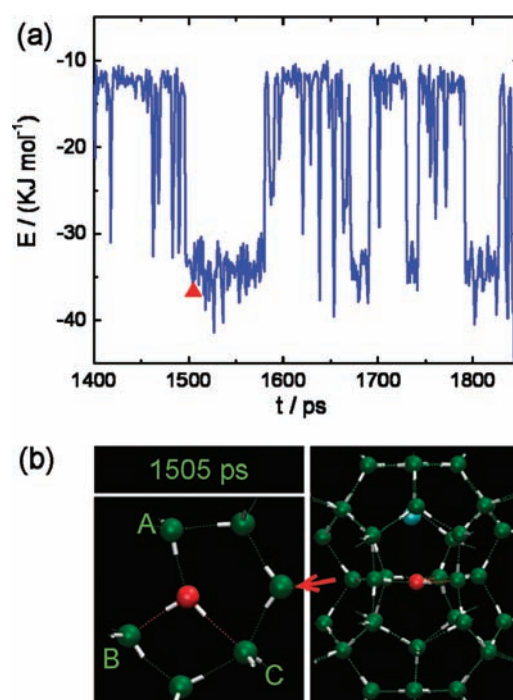


Figure 5. (a) Potential energy of an interstitial H₂O molecule in a $S^{12}6^2$ cage as a function of time. (b) An example of a molecular arrangement when this interstitial molecule has inserted itself into the center of a six-membered ring (the corresponding time has been labeled with the red triangle in (a)). CH₄ molecules are represented by light blue spheres, and H₂O molecules are represented as in Figure 1. The molecular labels “A”, “B”, and “C” are discussed in the text.

neighboring (H-bonded) H₂O molecules (“A” and “B” in Figure 4b) of the five-membered ring. As a result, a six-membered ring formed (Figure 4b). Since this six-membered ring does not conform to the hydrate crystal structure, the H-bonds between its molecules are destabilized. In some cases, the H-bond between molecules “B” and “C” is broken and molecule “C” escapes the six-membered ring (see Figure 4c). The remaining molecules reform the five-membered ring with little subsequent movement leaving the defect within a new cage (see Figure 4d). The behavior of the potential energy change of the H₂O molecules is similar to that observed in Figure 3.

3.2. Transport via Six-Membered Rings. Our MD simulations show that if the interstitial molecules are trapped in $S^{12}6^2$ cages, these defect molecules have a strong tendency to interact with one of the two six-membered rings of their host cage, rather than staying exclusively at the center of the cage. Figure 5a presents a typical example of the potential energy for an interstitial H₂O molecule trapped in a $S^{12}6^2$ cage as a function of simulation time. Two distinct potential energy values are apparent. The higher energy level corresponds to when the H₂O molecule is located at (or near) the center of the cage. The lower energy level, which is still substantially higher than the value of cage-forming molecules, corresponds to when the H₂O molecule has inserted itself into the center of one of the six-membered rings of the $S^{12}6^2$ cage (an example of the molecular configuration is shown in Figure 5b). At a temperature of 265 K, we observe the interstitial molecule regularly hopping between the center of the cage and center of a six-membered ring. For any particular molecule, one observes the associated potential energy fluctuations until it eventually becomes a cage-forming molecule

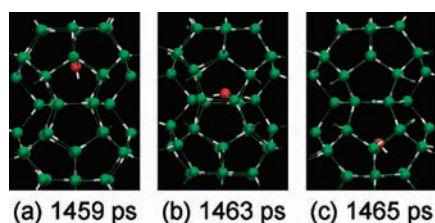


Figure 6. Process of a H_2O molecule hopping through the shared six-membered ring between two neighboring $S^{12}6^2$ cages (a–c). The corresponding time indexes for these configurations are given in the legends. The molecules are represented as in the case of Figure 1.

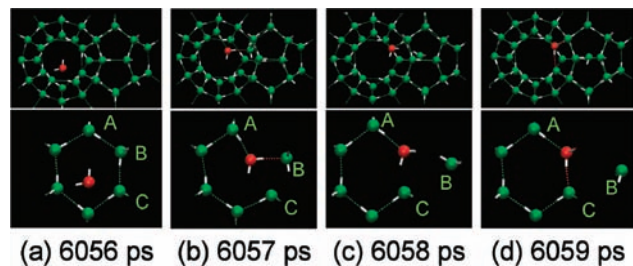


Figure 7. Molecular configurations (top) and corresponding ring structures (bottom) showing the mechanism of H_2O molecule transport from a $S^{12}6^2$ cage to a neighboring S^{12} cage via replacement of a H_2O molecule in a six-membered ring. The corresponding time indices for these configurations are given in the legends. H_2O molecules are represented as in the case of Figure 1. The molecular labels “A”, “B”, and “C” are discussed in the text.

(in the case of the molecule in Figure 5, after about 1850 ps). Figure 5b indicates that when the interstitial H_2O molecule inserts into a six-membered ring, it breaks one H-bond (between molecules “A” and “B”) of the original six-membered ring and forms three new H-bonds with the molecules of the ring. This arrangement of the H_2O molecules (ring plus interstitial) is in fact the most stable configuration at low temperature (see SI). At 265 K, we find that an interstitial H_2O molecule within a $S^{12}6^2$ cage spends about 40% of its total time inserted into a six-membered ring, where an insertion event might typically span tens of picoseconds, indicating that the free energy of the interstitial molecule is only slightly lower when it is at the center of the cage.

The structural arrangement shown in Figure 5b can result in two distinct pathways for the transport of a H_2O molecule. If the six-membered ring happens to be shared with an empty $S^{12}6^2$ cage, then the interstitial H_2O molecule readily hops between the two $S^{12}6^2$ cages through the shared six-membered ring. Figure 6 shows an example of such an event. An example of the potential energy change of the interstitial H_2O molecule during this hopping process can be found in the SI. There is apparently no energy barrier for the H_2O hopping through the six-membered ring; indeed the energy of the interstitial molecule exhibits a minimum, although there is a very slightly free energy barrier (at 265 K).

A second observed pathway resulting from the arrangement shown in Figure 5b is presented in Figure 7. In this case there is a replacement of a molecule of the six-membered ring by the interstitial H_2O molecule, thereby allowing the defect molecule to be transported into a neighboring empty S^{12} cage (see Figure 7a). The two cages involved share a pentagonal face which

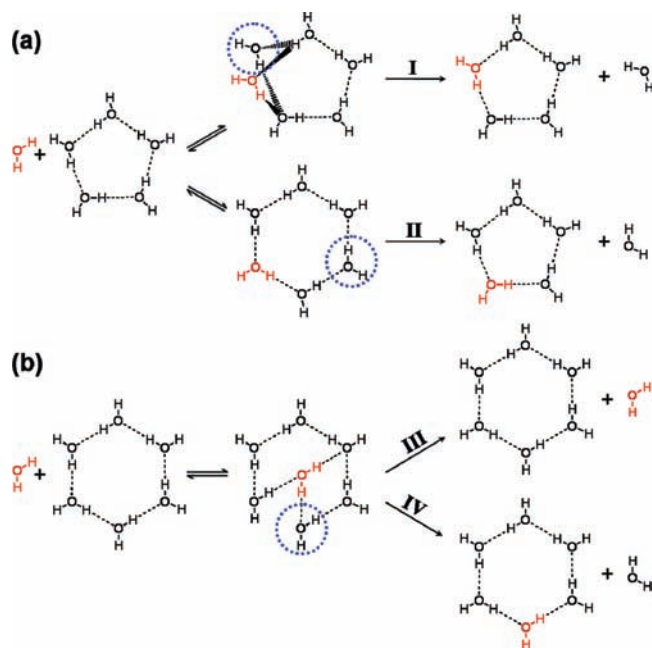


Figure 8. Schematic representation of four distinct pathways for interstitial H_2O molecule transport within hydrate crystals. (a) Transport by replacement of a molecule in a five-membered ring through H-bond formation with two second-neighbor molecules (pathway I) and with two neighboring molecules of the ring (thus forming a six-membered ring, pathway II). (b) Transport by interacting with six-membered rings via hopping through the ring (pathway III) and by replacement of a molecule of the ring (pathway IV). The circled molecules typically leave the ring during transport mechanisms I, II, and IV.

includes one edge of the six-membered ring (B–C; see Figure 7a). When the interstitial molecule inserts into the center of the six-membered ring, one H-bond (A–B; see Figure 7b) is broken. As a result of thermal fluctuations, another H-bond (B–C) is broken, resulting in a dangling H_2O molecule (B) originally from the six-membered ring (see Figure 7c). This molecule is now inside the previously empty S^{12} cage. Subsequent movement of the remaining molecules reforms the six-membered ring, leaving no defect in the host structures (see Figure 7d).

3.3. Water Transport Pathways. All the simulations at different temperatures from 245 to 275 K show similar transport mechanisms. Figure 8 summarizes the four distinct pathways for the transport of an interstitial defect molecule through gas hydrate crystals. The two transport pathways that proceed by replacement of a H_2O molecule within a five-membered ring are shown in Figure 8a. Since an interstitial H_2O molecule has a relatively high energy, it can attach itself to two first- or second-neighbor molecules of a five-membered ring and form a transient bridging structure (pathway I) or a six-membered ring (pathway II). From either of the intermediate structures, replacement of one of the molecules from the original five-membered ring is then possible. Through these two pathways, a H_2O molecule defect can be transported from one cage to either an empty first- or second-neighbor cage.

The two transport pathways that involve six-membered rings are shown in Figure 8b. As noted above, interstitial molecules trapped in $S^{12}6^2$ cages have a strong tendency to insert themselves into the center of one of the six-membered rings of their

Table 1. Number of Transport Events Observed during 12 ns Simulations at Temperatures of 265 and 275 K

	Path I	Path II	Path III	Path IV
265 K	6	7	3	2
275 K	12	11	4	2

host cage, this tendency increasing as the temperature is reduced. Such a structural arrangement can result in the hopping of interstitial molecules through the six-membered ring (pathway III) or the replacement of a molecule of the six-membered ring by the interstitial molecule (pathway IV).

The transport pathways reported here allow an interstitial H₂O molecule defect to transport from one cage to any empty cage that is a cage's first- and second-neighbor (for a 5¹² cage in an sI hydrate, this is 32 cages). Considering that the level of vacant cages in natural gas hydrates can be as high as 10%,^{32–34} one could expect the probability of an interstitial H₂O molecule being stranded in a fully occupied environment to be rather low. In other words, by the mechanisms presented above, interstitial H₂O defects could diffuse rather easily through hydrate crystals. The fact that the diffusion of interstitial H₂O molecules is facilitated by the vacancy cages suggests that some hydrates (like the sII tetrahydrofuran hydrate) with all the small cages being vacant could have an enhanced mobility of interstitial H₂O molecules.

In the present 50 ns of simulation, or indeed in hundreds of nanoseconds in our previous crystal growth simulations of gas hydrates,^{29–32,35,36} we have not observed formation of a lattice vacancy. This suggests that the diffusion of interstitial H₂O molecules, apparently facilitated by the existence of empty cages in hydrate crystals, may dominate lattice vacancies as a mechanism for the mass transfer of H₂O molecules through gas hydrates. This conjecture is supported by the experimental observation that there is a small but non-negligible population of interstitial H₂O defects in hexagonal ice and that the migration of these interstitial molecules provides the mechanism by which diffusion occurs in ice.^{37–39}

3.4. Temperature Dependence and Other Implications.

From our MD simulations at temperatures of 265 and 275 K, the numbers of observed transport events by the four pathways (see Figure 8) are presented in Table 1. While simulations were performed at lower temperatures, 245 and 255 K, the overall observed number of transport events was found to be very small and hence these data were not considered for further analysis. We do point out, however, that these limited data do show essentially no temperature dependence of the transport by pathway III, consistent with the suggestion of essentially no free energy barrier associated with transport by this pathway. We again point out that in simulations at low temperatures the interstitial molecule stays very close to the center of the ring (see SI), confirming that there is no energy barrier involved in this pathway.

From Table 1, we can also see that at these temperatures the transport of interstitial H₂O molecules is apparently dominated by pathways I and II, consistent with the fact that the number of five-membered rings is eight times larger than that of six-membered rings in sI hydrates. Assuming Arrhenius-type behavior for the temperature dependence exhibited by pathways I and II, we can roughly estimate an effective (free) energy barrier of around 30 kJ·mol⁻¹ for diffusion by the two pathways. This estimate is reasonably consistent with that of ice Ih

(15.4 kJ·mol⁻¹),⁴⁰ considering that the apparent activation energy for gas and H₂O transport through hydrates measured experimentally by Kuhs et al.¹⁸ is also larger than that for diffusion of H₂O molecules in ice. We note that a more precise determination of the free energy barrier by the current simulation method would be rather difficult, requiring extensive averaging to allow for sampling over the varied behavior of each transport event (as noted above).

If we assume that the movements of interstitial H₂O molecules within a crystal can be described with a random-walk model, then the diffusion coefficient, D_p , of these interstitial defects can be estimated to be about 1×10^{-10} and 2×10^{-10} m²/s at temperatures of 265 and 275 K, respectively. Here we have assumed that the length of each step is the distance between the centers of neighboring cages, and the time step is approximated from the event data in Table 1. These diffusion coefficients of interstitial molecules in hydrates are comparable with that of ice (as derived from the X-ray topographic studies⁴¹). Based on (limited) data from crystal growth simulations of CH₄ hydrates at temperatures 10–20 K below their melting temperature,^{30,32} the concentration, n_i/N , of interstitial water molecules is of the order of 0.1%. From these values the coefficient of the self-diffusion, D_s , of H₂O molecules by interstitial mechanisms can then be estimated to be about 10⁻¹³ m²/s (using $D_s = (n_i/N)D_i$ ⁴¹). This estimate agrees well with recent in situ high-resolution confocal Raman spectroscopy studies,²⁵ which predict an effective diffusivity of H₂¹⁸O tracers through hydrate films of about 10⁻¹³ m²/s under comparable conditions.

The H₂O transport pathways discussed above suggest that other H-bonding guests such as small ethers, H₂S, etc., may also have an enhanced mobility in gas hydrates. It has been reported that hydrates can form at remarkably fast rates with H-bonding guests,^{15,42} suggesting the rapid transport of such H-bonding guest molecules within hydrate films. The possible influence of H₂O diffusion on guest diffusion is also of potential importance. Previous studies have shown that guest molecules hopping through intact five- and six-membered H₂O rings would experience substantial energy barriers,^{23,24} with the exception of very small molecules like H₂.⁴³ Based on those results, one might infer that guest molecule diffusion is dependent upon defects in the host lattices. Since interstitial H₂O molecules are able to generate structural defects within the host lattice, one might envisage that guest molecules could take advantage of such temporary defective structures to hop from one cage to another. Unfortunately, we have not observed a guest molecule (CH₄ or H₂S) hopping event during our simulations. This may be because the time scale of the current MD simulation was simply not enough or may reflect a limitation of the (nonpolarizable) potential models used in this work. It is important to point out that similar H₂O transport processes in a H₂S hydrate have been observed in our MD simulations (see SI).

4. CONCLUSION

In this work, we report preliminary observations of the molecular transport of interstitial H₂O molecules through cages of gas hydrate crystals. Molecular simulations were utilized to explore and analyze the microscopic behavior of this process. Four distinct mechanisms, involving either five- or six-membered rings within cages, are presented and discussed. Results from two different temperatures yield an effective (free) energy barrier of around 30 kJ·mol⁻¹ for the diffusion of an interstitial defect

through five-membered rings (pathways I and II). The diffusion through six-membered rings (pathways III and IV) appears rather temperature insensitive, suggesting there is a negligible (free) energy barrier associated with these processes. For three of the transport pathways, the transition state structures represent the most stable arrangements at low temperatures. The estimated self-diffusion coefficient of H₂O molecules through a hydrate is consistent with values estimated from experiments.

This work proposes molecular mechanisms accounting for the apparent high mobility of H₂O through hydrate phases as observed experimentally. The relative richness of the behavior of interstitial defects determined in our study suggests that the diffusion of interstitial molecules could be an important mechanism for the mass transfer of H₂O through gas hydrates. To help characterize the transport processes uncovered here, further investigations into several aspects would appear warranted. Improved statistics for the concentration of interstitials are needed for a more quantitative analysis of the self-diffusion coefficient of the H₂O molecules. As noted above, the direct measurement of the free energy barrier of the processes is a challenge since the detailed behavior for each transport event varies due to molecular fluctuations. Other techniques (e.g., path sampling,⁴⁴ metadynamics⁴⁵) are perhaps required for an accurate description of the (average) energetics of these transport processes. It would also be useful to validate the transport mechanisms using different force fields (e.g., with polarizable or ab initio determined potentials^{46,47}). We hope this report will stimulate experimental efforts aimed at confirming the presence of a low concentration of interstitial H₂O molecules in (appropriately prepared) gas hydrate crystals and determining whether the self-diffusion of H₂O molecules through gas hydrates occurs by the processes described here or some other possible mechanism.

■ ASSOCIATED CONTENT

S Supporting Information. The Supporting Information contains further details on the simulation methodologies, the energies of molecules during the H₂O transport process, the stable structures of interstitial H₂O molecules trapped in 5¹² and 5¹²6² cages from low temperature simulations, and H₂O transport through H₂S hydrate crystals. This material is available free of charge via the Internet at <http://pubs.acs.org>.

■ AUTHOR INFORMATION

Corresponding Author
peter.kusalik@ucalgary.ca

■ ACKNOWLEDGMENT

We are grateful for the financial support of the Natural Sciences and Engineering Research Council of Canada. We also acknowledge computational resources made available via West-Grid (www.westgrid.ca) and the University of Calgary.

■ REFERENCES

- (1) Sloan, E. D.; Koh, C. A. *Clathrate hydrates of natural gases*; CRC Press: Boca Raton, FL, 2007.
- (2) Sloan, E. D. *Nature* **2003**, *426*, 353.
- (3) Myshakin, E. M.; Jiang, H.; Warzinski, R. P.; Jordan, K. D. *J. Phys. Chem. A* **2009**, *113*, 1913.

- (4) Park, Y.; Kim, D. Y.; Lee, J. W.; Huh, D. G.; Park, K. P.; Lee, J.; Lee, H. *Proc. Natl. Acad. Sci. U.S.A.* **2006**, *103*, 12690.
- (5) Ota, M.; Morohashi, K.; Abe, Y.; Watanabe, M.; Smith, R. L.; Inomata, H. *Energy Conv. Manag.* **2005**, *46*, 1680.
- (6) Strobel, T. A.; Kim, Y.; Andrews, G. S.; Ferrell, J. R.; Koh, C. A.; Herring, A. M.; Sloan, E. D. *J. Am. Chem. Soc.* **2008**, *130*, 14975.
- (7) Lee, H.; Lee, J. W.; Kim, D. Y.; Park, J.; Seo, Y. T.; Zeng, H.; Moudrakovski, I. L.; Ratcliffe, C. I.; Ripmeester, J. A. *Nature* **2005**, *434*, 743.
- (8) Florusse, L. J.; Peters, C. J.; Schoonman, J.; Hester, K. C.; Koh, C. A.; Dec, S. F.; Marsh, K. N.; Sloan, E. D. *Science* **2004**, *306*, 469.
- (9) Svensen, H.; Planke, S.; Malthes-Sorensen, A.; Jamtveit, B.; Myklebust, R.; Eidem, T. R.; Rey, S. S. *Nature* **2004**, *429*, 542.
- (10) Hesselbo, S. P.; Grocke, D. R.; Jenkyns, H. C.; Bjerrum, C. J.; Farrimond, P.; Bell, H. S. M.; Green, O. R. *Nature* **2000**, *406*, 392.
- (11) Kennedy, M.; Mrofk, D.; von der Borch, C. *Nature* **2008**, *453*, 642.
- (12) Archer, D.; Buffett, B.; Brovkin, V. *Proc. Natl. Acad. Sci. U.S.A.* **2009**, *106*, 20596.
- (13) Kvenvolden, K. A. *Proc. Natl. Acad. Sci. U.S.A.* **1999**, *96*, 3420.
- (14) Kleinberg, R. L.; Flaum, C.; Griffin, D. D.; Brewer, P. G.; Malby, G. E.; Peltzer, E. T.; Yesinowski, J. P. *J. Geophys. Res.-Solid Earth* **2003**, *108*, 2508.
- (15) Buch, V.; Devlin, J. P.; Monreal, I. A.; Jagoda-Cwiklik, B.; Uras-Aytemiz, N.; Cwiklik, L. *Phys. Chem. Chem. Phys.* **2009**, *11*, 10245.
- (16) Moudrakovski, I. L.; McLaurin, G. E.; Ratcliffe, C. I.; Ripmeester, J. A. *J. Phys. Chem. B* **2004**, *108*, 17591.
- (17) Taylor, C. J.; Dieker, L. E.; Miller, K. T.; Koh, C. A.; Sloan, E. D. *J. Colloid Interface Sci.* **2007**, *306*, 255.
- (18) Staykova, D. K.; Kuhs, W. F.; Salamatin, A. N.; Hansen, T. *J. Phys. Chem. B* **2003**, *107*, 10299.
- (19) Henning, R. W.; Schultz, A. J.; Thieu, V.; Halpern, Y. *J. Phys. Chem. A* **2000**, *104*, 5066.
- (20) Teng, H.; Yamasaki, A.; Shindo, Y. *Chem. Eng. Sci.* **1996**, *51*, 4979.
- (21) Shindo, Y.; Fujioka, Y.; Takeuchi, K.; Komiyama, H. *Int. J. Chem. Kinet.* **1995**, *27*, 569.
- (22) Mori, Y. H.; Mochizuki, T. *Chem. Eng. Sci.* **1997**, *52*, 3613.
- (23) Demurov, A.; Radhakrishnan, R.; Trout, B. L. *J. Chem. Phys.* **2002**, *116*, 702.
- (24) Peters, B.; Zimmermann, N. E. R.; Beckham, G. T.; Tester, J. W.; Trout, B. L. *J. Am. Chem. Soc.* **2008**, *130*, 17342.
- (25) Davies, S. R.; Sloan, E. D.; Sum, A. K.; Koh, C. A. *J. Phys. Chem. C* **2010**, *114*, 1173.
- (26) Kirschgen, T. M.; Zeidler, M. D.; Geil, B.; Fujara, F. *Phys. Chem. Chem. Phys.* **2003**, *5*, 5247.
- (27) Uchida, T.; Takeya, S.; Wilson, L. D.; Tulk, C. A.; Ripmeester, J. A.; Nagao, J.; Ebinuma, T.; Narita, H. *Can. J. Phys.* **2003**, *81*, 351.
- (28) Kuhs, W. F.; Staykova, D. K.; Salamatin, A. N. *J. Phys. Chem. B* **2006**, *110*, 13283.
- (29) Liang, S.; Kusalik, P. G. *J. Phys. Chem. B* **2010**, *114*, 9563.
- (30) Liang, S.; Kusalik, P. G. *Chem. Phys. Lett.* **2010**, *494*, 123.
- (31) Vatamanu, J.; Kusalik, P. G. *J. Phys. Chem. B* **2008**, *112*, 2399.
- (32) Vatamanu, J.; Kusalik, P. G. *J. Phys. Chem. B* **2006**, *110*, 15896.
- (33) Uchida, T.; Hirano, T.; Ebinuma, T.; Narita, H.; Gohara, K.; Mae, S.; Matsumoto, R. *Aiche J.* **1999**, *45*, 2641.
- (34) Huo, Z. X.; Hester, K.; Sloan, E. D.; Miller, K. T. *Aiche J.* **2003**, *49*, 1300.
- (35) Vatamanu, J.; Kusalik, P. G. *J. Chem. Phys.* **2007**, *126*, 124703.
- (36) Vatamanu, J.; Kusalik, P. G. *J. Am. Chem. Soc.* **2006**, *128*, 15588.
- (37) Itagaki, K. *J. Phys. Soc. Jpn.* **1967**, *22*, 427.
- (38) Ramseier, R. O. *J. Appl. Phys.* **1967**, *38*, 2553.
- (39) Hondoh, T.; Itoh, T.; Higashi, A. *Jpn. J. Appl. Phys.* **1981**, *20*, L737.
- (40) Hondoh, T. *Glide and climb processes of dislocations in ice. In Physics and Chemistry of Ice*; Maeno, N., Hondoh, T., Eds.; Hokkaido University Press: Sapporo, Japan, 1992; p 481.

- (41) Petrenko, V. F.; Whitworth, R. W. *Physics of Ice*; Oxford University Press: Oxford, U.K., 1999.
- (42) Devlin, J. P.; Monreal, I. A. *Chem. Phys. Lett.* **2010**, *492*, 1.
- (43) Alavi, S.; Ripmeester, J. A. *Angew. Chem., Int. Ed.* **2007**, *46*, 6102.
- (44) Bolhuis, P. G.; Chandler, D.; Dellago, C.; Geissler, P. L. *Annu. Rev. Phys. Chem.* **2002**, *53*, 291.
- (45) Laio, A.; Parrinello, M. *Proc. Natl. Acad. Sci. U.S.A.* **2002**, *99*, 12562.
- (46) Cui, J.; Liu, H. B.; Jordan, K. D. *J. Phys. Chem. B* **2006**, *110*, 18872.
- (47) Jiang, H.; Jordan, K. D.; Taylor, C. E. *J. Phys. Chem. B* **2007**, *111*, 6486.